Dalton Transactions

PAPER

View Article Online
View Journal

Cite this: DOI: 10.1039/c4dt02969k

Rhenium and technetium complexes that bind to amyloid-β plaques†

David J. Hayne,[a,b] Andrea J. North,[a,b] Michelle Fodero-Tavoletti,[c,e] Jonathan M. White,[a,b] Lin W. Hung,[b,c] Angela Rigopoulos,[d] Catriona A. McLean,[c,f] Paul A. Adlard,[c] Uwe Ackermann,[e] Henri Tochon-Danguy,[e] Victor L. Villemagne,[c,e] Kevin J. Barnham[b,c,g] and Paul S. Donnelly*[a,b]

Received 26th September 2014,
Accepted 2nd December 2014

DOI: 10.1039/c4dt02969k

www.rsc.org/dalton

Alzheimer's disease is associated with the presence of insoluble protein deposits in the brain called amyloid plaques. The major constituent of these deposits is aggregated amyloid-β peptide. Technetium-99m complexes that bind to amyloid-β plaques could provide important diagnostic information on amyloid-β plaque burden using Single Photon Emission Computed Tomography (SPECT). Tridentate ligands with a stilbene functional group were used to form complexes with the *fac*-$[M^{I}(CO)_3]^+$ (M = Re or ^{99m}Tc) core. The rhenium carbonyl complexes with tridentate co-ligands that included a stilbene functional group and a dimethylamino substituent bound to amyloid-β present in human frontal cortex brain tissue from subjects with Alzheimer's disease. This chemistry was extended to make the analogous $[^{99m}Tc^{I}(CO)_3]^+$ complexes and the complexes were sufficiently stable in human serum. Whilst the lipophilicity (log $D_{7.4}$) of the technetium complexes appeared ideally suited for penetration of the blood-brain barrier, preliminary biodistribution studies in an AD mouse model (APP/PS1) revealed relatively low brain uptake (0.24% ID g^{-1} at 2 min post injection).

Introduction

Alzheimer's disease (AD) is the major cause of neurodegenerative dementia. A pathological hallmark of the disease is the presence of extracellular senile plaques in the brain. The major constituent of these plaques is an aggregated peptide called amyloid-β (Aβ), a 39–43 amino acid peptide derived from the amyloid precursor protein (APP).[1,2] The exact role of Aβ plaques in dementia remains controversial, but extensive cortical Aβ deposition is a common feature identified by post-mortem analysis of AD subjects.[3] Clinical diagnosis of AD relies on tests to establish progressive impairment of memory and in at least one other area of cognition.[4,5] Molecular imaging techniques offer the possibility of identifying disease associated pathology and the desire for earlier and more accurate diagnosis of AD has led to the development of radioactive tracers designed to cross the blood-brain barrier and bind with some degree of selectivity to Aβ plaques.

The fluorescent dye Thioflavin-T that binds to Aβ plaques *in vitro* provided the structural inspiration for the development of several radiolabelled benzothiazole and stilbene compounds that have been used with considerable success to quantify plaque burden in human patients. It is thought that these molecules enter a hydrophobic pocket or channel and bind to the plaques by way of a combination of hydrophobic and π–π interactions. The benzothiazole, 2-(4-[^{11}C]methylamino-phenyl)-6-hydroxybenzo-thiazole, known as Pittsburgh compound-B or [^{11}C]PiB (Fig. 1), makes use of the short-lived positron-emitting isotope ^{11}C to enable diagnostic imaging using positron emission tomography (PET).[6–8] There are some similarities in the chemical structure of benzothiazoles, such as PiB, and other plaque targeting groups such as stilbenes, in that they have conjugated aromatic ring systems and are relatively planar molecules. A variety of stilbene and styrylpyridine derivatives are excellent probes for Aβ plaques and a stilbene derivative radiolabelled with carbon-11 (4-*N*-methylamino-4′-hydroxystilbene), known as SB-13 (Fig. 1), binds selectively to

[a]School of Chemistry, University of Melbourne, Melbourne, 3010, Australia. E-mail: pauld@unimelb.edu.au
[b]Bio21 Molecular Science and Biotechnology Institute, 30 Flemington Road, The University of Melbourne, Victoria 3010, Australia
[c]Florey Institute of Neuroscience and Mental Health, University of Melbourne, Parkville, Melbourne, Victoria 3010, Australia
[d]Ludwig Institute for Cancer Research, Heidelberg, Victoria, Australia
[e]Department of Molecular Imaging and Therapy, Austin Health, Melbourne, Heidelberg, Victoria 3084, Australia
[f]Department of Anatomical Pathology, The Alfred Hospital, Victoria 3181, Australia
[g]Department of Pharmacology, University of Melbourne, Parkville, Melbourne, Heidelberg, Victoria 3084, Australia

† Electronic supplementary information (ESI) available: Images of tissue sections from the frontal cortex of an age-matched control brain treated with $[Re(CO)_3\mathbf{L}^2]$ and $[Re(CO)_3\mathbf{L}^4]$. CCDC 1025768 and 1025769. For ESI and crystallographic data in CIF or other electronic format see DOI: 10.1039/c4dt02969k

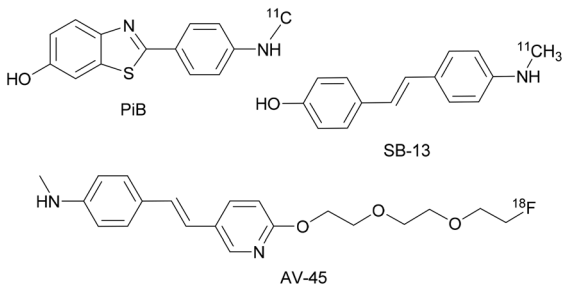

Fig. 1 Chemical structures of [^{11}C]PiB, SB-13 and ^{18}F-AV45.

Aβ plaques.[3,9,10] Preliminary studies of SB-13 in humans were promising and stimulated continued explorations of stilbene and styrylpyridine derivatives, as probes for Aβ plaques.[3,11] The longer half-life of fluorine-18 when compared to carbon-11 (^{11}C = 20.4 min, ^{18}F = 109.7 min) encouraged efforts to develop stilbene[12] or styrylpyridine[13,14] derivatives radiolabelled with fluorine-18 culminating in the recent FDA approval of ^{18}F-AV45 (florbetapir) (Fig. 1) to detect the presence of amyloid.[3,5,15–17]

For imaging applications using carbon-11 or fluorine-18 radioisotopes the isotopes are produced by cyclotrons and the radionuclides are attached covalently to plaque binding molecules. Covalent attachment of radioisotopes to tracers requires complicated synthetic manipulations and specialist equipment. Despite the rapid increase in the number of hospitals equipped with the requisite infrastructure for PET, single photon emission computed tomography (SPECT) is the most commonly used nuclear imaging technique. The most commonly used radioisotope for SPECT is ^{99m}Tc, which is available from convenient generators. The 6 hour half-life of ^{99m}Tc is sufficiently long to allow for the preparation of pure technetium complexes and for accumulation in target tissue, but short enough to not deliver excessive radiation doses to the patient. A ^{99m}Tc based radiotracer for determining plaque burden suitable for SPECT imaging would be of considerable clinical utility by increasing the number of centres that are able to perform diagnostic scans.[18–20] Several technetium complexes based on tetradentate N_2S_2 ligands fused to phenylbenzothiazole plaque binding groups designed to form neutral complexes with the $[Tc^{V}O]^{3+}$ have been synthesized. Some of these $[Tc^{V}O]^{3+}$ complexes show considerable promise and warrant further investigation.[20–22] An alternative technetium 'core' to the $[Tc^{V}O]^{3+}$ is the low valent $[Tc^{I}(CO)_3]^{+}$ and innovations in synthetic methodology have led to the possibility of preparing *fac*-$[M(CO)_3(H_2O)_3]^{+}$ (where M = Tc^{I} or Re^{I}) using conditions amenable to radiopharmaceutical applications.[23–25] The "carbonyl core" approach exploits the stability of the metal tricarbonyl core by substituting the water ligands with ligands designed to modify biodistribution. In the absence of non-radioactive isotopes of technetium the Group VII congener rhenium, which by virtue of the lanthanide contraction has similar ionic radii to technetium, is often used as a surrogate to guide synthetic developments. This manuscript describes the synthesis and characterisation of tridentate ligands designed to bind to the $[M(CO)_3]^{+}$ core (M = Tc^{I}/Re^{I}) that feature pendent stilbene functional groups designed to bind to amyloid plaques. The ability of the new rhenium complexes to bind to Aβ plaques in human brain tissue is assessed and the preliminary brain uptake of the ^{99m}Tc analogues is determined in both wild-type mice and a mouse model of Aβ plaque pathology (APP/PS1).

Results and discussion

Synthesis and characterisation

The *fac*-$[M(CO)_3(H_2O)_3]^{+}$ (M = Tc^{I}/Re^{I}) cation can be considered a "semi metal aqua cation" where the carbonyl ligands stabilize the low oxidation state and the *trans* effect increases the lability of coordinated water molecules. Ligands containing an aromatic amine and carboxylate donors coordinate to *fac*-$[M(CO)_3]^{+}$ with rapid complexation kinetics producing complexes with good stability in aqueous solvents. Tridentate ligands bearing two pyridyl groups such as dipicolylamine serve as a versatile and useful starting point for bifunctional ligands where the amine nitrogen can be used to tether targeting groups. In this manuscript we present the synthesis of two pyridylamine-carboxylate tridentate ligands (H$\mathbf{L^1}$, H$\mathbf{L^2}$) and two dipyridylamine ligands ($\mathbf{L^3}$, $\mathbf{L^4}$) that each feature stilbene-like functional groups connected by a short alkyl linker (Fig. 2).

The synthesis of the tridentate ligands H$\mathbf{L^2}$ and $\mathbf{L^4}$ utilised aldehyde **2**, (*E*)-4-(4-*N*,*N*-dimethylaminostyryl)benzaldehyde, that was prepared by formylation of *E*-4-(4-bromostyryl)-*N*,*N*-dimethylaniline (**2a**). Precursor **2a** was prepared by a Horner–Wadsworth–Emmons reaction between diethyl-4-bromobenzylphosphonate and 4-*N*,*N*-dimethylaminobenzaldehyde (Scheme 1). The methyl ester of $\mathbf{L^1}$ was prepared by reductive amination of 2-picolylamine with *E*-4-stilbenecarboxaldehyde (**1**) to give pyridyl amine **3** followed by an aza-Michael addition with methyl acrylate (Scheme 2). The synthesis of $\mathbf{L^3}$ involved aza-Michael addition between pyridyl amine **3** and 2-vinylpyridine. Reductive amination of aldehyde **2** with 2-picolylamine followed by aza-Michael additions with either methyl acrylate or 2-vinylpyridine furnished either the methyl ester of $\mathbf{L^2}$ or $\mathbf{L^4}$

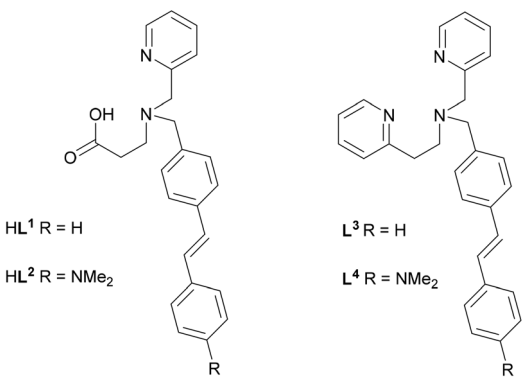

Fig. 2 Chemical structures of ligands $H_2\mathbf{L^{1-2}}$ and $\mathbf{L^{3-4}}$.

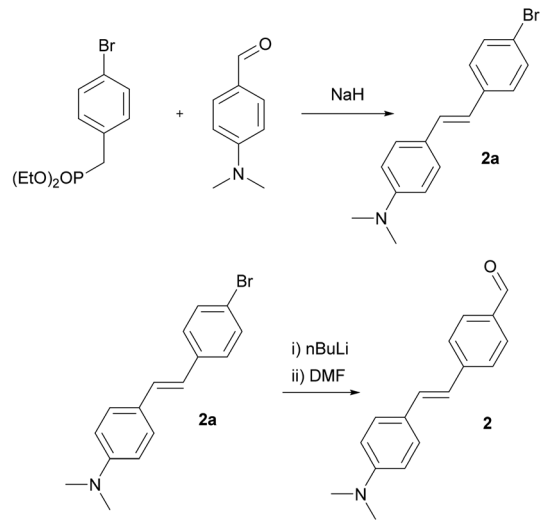

Scheme 1 Synthesis of precursor **2a** by Wadsworth-Emmons-Horner reaction followed by formylation of **2a** to give aldehyde **2**.

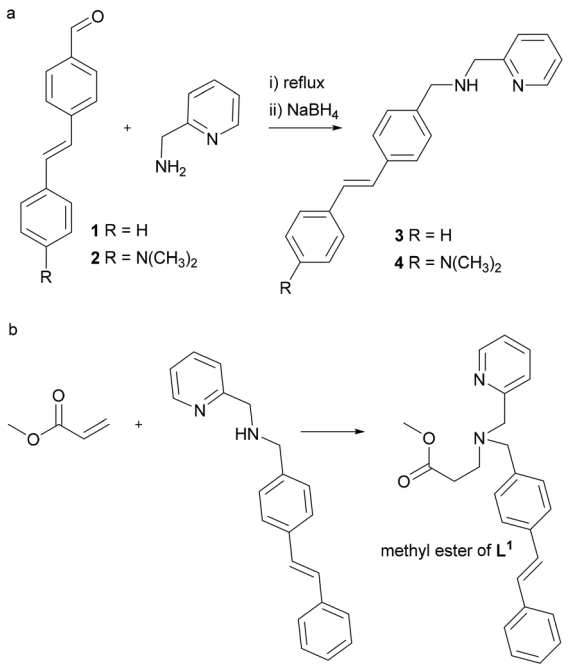

Scheme 2 (a) Reductive amination of (*E*)-stilbene-carboxyaldehyde derivatives (aldehydes **1** or **2**) to give pyridylamines **3** or **4** respectively. (b) Synthesis of proligand Me$\mathbf{L^1}$ by aza-Michael addition of **3** with methyl acrylate.

(Scheme 2). The methyl esters of $\mathbf{L^1}$ and $\mathbf{L^2}$, were hydrolysed to give the corresponding carboxylic acids, H$\mathbf{L^1}$ and H$\mathbf{L^2}$.

The rhenium complexes *fac*-[$Re^I(CO)_3\mathbf{L^{1-2}}$] and *fac*-[$Re^I(CO)_3\mathbf{L^{3-4}}]^+$ were prepared by microwave irradiation of an aqueous mixture of [$Re^I(CO)_5(CF_3SO_3)$] with the respective ligands in methanol. The use of microwave irradiation offers the advantage of high product yields with relatively short reaction times of about 30 minutes. For each complex, analysis by

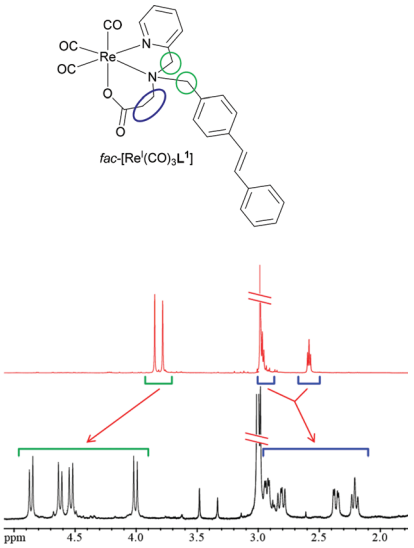

Fig. 3 ^{1}H NMR spectra of Me$\mathbf{L^1}$ (red) and *fac*-[$Re^I(CO)_3\mathbf{L^1}$] (black). Methylene protons and signals are highlighted with green marks and ethylene with blue.

^{1}H NMR spectroscopy confirmed the *E*-stereochemistry of the stilbene pendant groups was retained ($^3J_{HH}$ > 16 Hz). Upon coordination to the metal the methylene and ethylene protons of each ligand become diasterotopic, for example, the ^{1}H NMR spectrum of the methyl ester of $\mathbf{L^1}$ has singlets for each of the two methylene groups and two multiplets for the proton pairs within the ethylene that split into in four AB doublets for each methylene proton and four multiplets for the ethylene protons upon coordination (Fig. 3).

The crystal structures of *fac*-[$Re^I(CO)_3\mathbf{L^1}$] and *fac*-[$Re^I(CO)_3\mathbf{L^3}]^+$ show distorted octahedral geometry about the metal centre with carbonyl groups arranged facially (Table 1). Compound *fac*-[$Re^I(CO)_3\mathbf{L^1}$] crystallises in the triclinic space group $P\bar{1}$ (Fig. 4). The asymmetric unit contains two neutral complexes and acetonitrile solvent molecules. In *fac*-[$Re^I(CO)_3\mathbf{L^1}$], the remaining coordination sphere of the metal is completed by an NNO donor atom set provided by the pyridyl nitrogen, tertiary amine and carboxylate groups of the ligand. The rhenium ion is in the equatorial plane defined by two carbonyl groups and the nitrogen donor atoms of the ligand with apical sites occupied by the remaining carbonyl group and carboxylato oxygen. Coordination of the ligand sees the formation of a five membered chelate ring containing two nitrogen donor atoms (N1, N2) and a methylene carbon (C6) and a six membered chelate ring that includes the two ethylene carbons (C7, C8), tertiary amine nitrogen (N2), and carboxylato oxygen (O1). The bond distances between rhenium and the two N donor atoms differ, with bond Re–N1 being 2.186(5) Å and Re–N2 2.262(5) Å in length. The Re–N1 bond length is within the range of similar *fac*-[$Re^I(CO)_3$NNO] complexes but bonds Re–O1 and Re–N2 are slightly longer, at 2.142(4) Å and 2.262(5) Å, compared to 2.107–2.132 Å and 2.232–2.255 Å respectively for similar complexes.[26–31] This is possibly due to the inclusion of a six

Table 1 Crystallographic data for *fac*-[Re^{I}(CO)$_3$**L^1**] or *fac*-[Re^{I}(CO)$_3$**L^3**]$^+$

	fac-[Re^{I}(CO)$_3$**L^1**]·0.5MeCN	*fac*-[Re^{I}(CO)$_3$**L^3**]-CF$_3$SO$_3$
Formula	$C_{28}H_{24.50}N_{2.50}O_5Re$	$C_{32}H_{27}F_3N_3O_6ReS$
M	662.20	824.82
Colour and Habit	Pink rod	Colourless block
Crystal size (mm^3)	0.13 × 0.06 × 0.04	0.36 × 0.27 × 0.21
System	Triclinic	Monoclinic
Space group	*P*$\bar{1}$	$P2_1/c$
T (°K)	130.0 K	130.0 K
a (Å)	10.6380(7)	13.3527(3)
b (Å)	12.5358(7)	14.7033(3)
c (Å)	19.0696(13)	17.0611(3)
α (°)	95.970(5)	90
β (°)	96.832(5)	91.244(2)
γ (°)	99.253(5)	90
U/Å^3	2472.4(3)	3348.79(12)
Z	4	4
D_{calcd} (Mg m^{-3})	1.779	1.636
Wavelength (Å)	1.5418 (Cu-Kα)	0.7107 (Mo-Kα)
Absorption coefficient (mm^{-1})	9.980	3.754
F(000)	1300	1624
Reflections measured	17 732	22 309
Independent reflections	9825 [R_{int} = 0.0456]	7471 [R_{int} = 0.0272]
R [$I > 2\sigma(I)$]	0.04	0.0378
w$R(F^2)$ (all data)	0.0525	0.0509

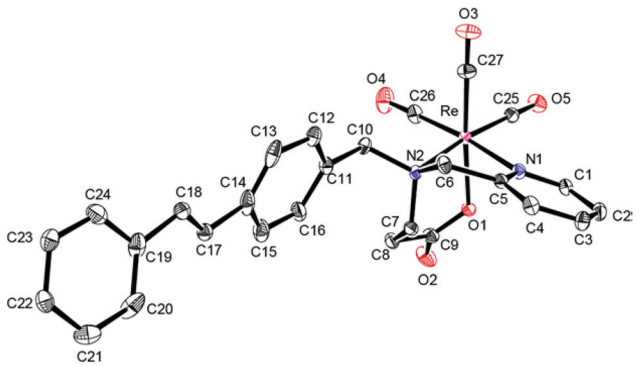

Fig. 4 An ORTEP representation of *fac*-[Re^{I}(CO)$_3$**L^1**] with 30% probability thermal ellipsoids, hydrogen atoms and solvent atoms omitted for clarity. Selected bond lengths (Å): Re–N1 2.186(5), Re–N2 2.262(5), Re–O1 2.142(4), Re–C25 1.927(7), Re–C26 1.913(7), Re–C27 1.928(7).

membered chelate ring instead of two five membered chelate rings seen in other complexes with the same donor atom set.

Compound *fac*-[Re^{I}(CO)$_3$**L^3**]$^+$ crystallises in the monoclinic space group $P2_1/c$ (Fig. 5). The asymmetric unit contains one cationic complex with the asymmetric ligand forming both a five and six membered chelate ring upon coordination. Bond Re–N3 (2.162(5) Å) is within the range of other *fac*-[Re^{I}(CO)$_3$]$^+$ complexes containing two pyridyl groups and a tertiary amine (Re–N_{py} = 2.155–2.187 Å) but Re–N1 is longer (2.213(4) Å). This is again likely due to the six membered chelate ring with the bond Re–N2 (2.251(4) Å) also being longer relative to similar complexes (Re–N_{amine} 2.216–2.242 Å).[26,27,32–36]

Ligands H**L$^{1-2}$** and **L$^{3-4}$** are fluorescent due to the presence of the stilbene functional group. The methyl ester of **L^1** and **L^3**

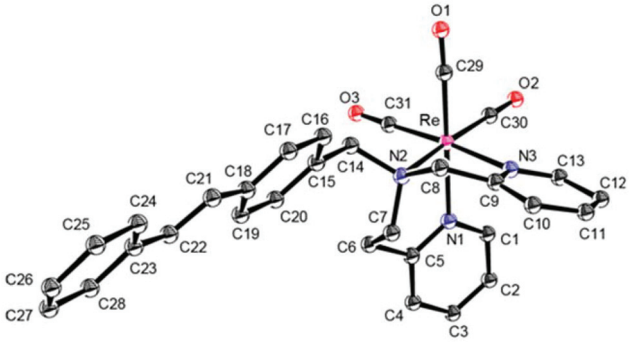

Fig. 5 An ORTEP representation of *fac*-[Re^{I}(CO)$_3$**L^3**]$^+$ with 30% probability thermal ellipsoids, disordered counterions ($^-$OTf) were removed by a squeeze procedure and hydrogen atoms are omitted for clarity. Selected bond lengths (Å): Re–N1 2.213(4), Re–N2 2.251(4), Re–N3 2.162(5), Re–C29 1.919(5), Re–C30 1.905(5), Re–C31 1.922(6).

have similar absorbance spectra each displaying two maxima at λ_{max} = 300 nm and λ_{max} = 312 nm. Both ligands fluoresce at λ_{em} = 355 nm following excitation at λ_{ex} = 312 nm. The absorbance spectra for *fac*-[Re^{I}(CO)$_3$**L^1**] and *fac*-[Re^{I}(CO)$_3$**L^3**]$^+$ have maxima at λ_{max} = 300 and λ_{max} = 312 nm, and an emission with a maximum at λ_{em} = 360 nm (Fig. 6a). There is an increase in molar absorptivity upon coordination, from 27.0(±0.2) × 10^3 M^{-1} cm^{-1} and 30.6(±0.3) × 10^3 M^{-1} cm^{-1} for the methyl ester of **L^1** and **L^3** respectively to 43.5(±0.9) × 10^3 M^{-1} cm^{-1} for *fac*-[Re^{I}(CO)$_3$**L^1**] and 42.9(±0.3) × 10^3 M^{-1} cm^{-1} for *fac*-[Re^{I}(CO)$_3$**L^3**]$^+$. The introduction of the electron donating dimethylamino functional group (H**L^2** and **L^4**) leads to a bathochromic shift of approximately 40 nm in the absorbance maxima (*λ* 355 nm for H**L^2**, *λ* 345 nm for H**L^4**) and larger Stokes shifts of 90–100 nm. Complexes *fac*-[Re^{I}(CO)$_3$**L^2**] and *fac*-[Re^{I}(CO)$_3$**L^4**]$^+$ are also fluorescent (λ_{em} = 472 nm for *fac*-[Re^{I}(CO)$_3$**L^2**] and *λ* 464 nm for *fac*-[Re^{I}(CO)$_3$**L^4**]$^+$ (Fig. 6b)). The electronic spectra of stilbene and its derivatives are concentration dependent leading to excimer formation and stilbenes are photochromic but such detail was not investigated for these derivatives.

Binding of *fac*-[Re^{I}(CO)$_3$L$^{1-2}$] & *fac*-[Re^{I}(CO)$_3$L$^{3-4}$]$^+$ to Aβ plaques in human brain tissue. Frontal cortex brain tissue collected from subjects with clinically diagnosed AD and age matched control subjects were used to determine the plaque-binding capacity of the new rhenium complexes. Amyloid-β plaques are typically 30–50 μm in diameter so 5 μm serial sections of tissue often contain comparable Aβ plaque distribution. Aβ plaques were stained with an Aβ antibody (1E8) and contiguous sections of brain tissue were treated with a solution of a chosen Re complex. The complexes *fac*-[Re^{I}(CO)$_3$**L^1**] or *fac*-[Re^{I}(CO)$_3$**L^3**]$^+$ showed little to no plaque binding within brain tissue from AD positive subjects. The complexes that contained the electron-donating dimethylamino functional group were more promising. Epifluorescent microscopy of tissue sections treated with *fac*-[Re^{I}(CO)$_3$**L^2**] and *fac*-[Re^{I}(CO)$_3$**L^4**]$^+$ reveal good correlation of the complexes to Aβ plaques stained with

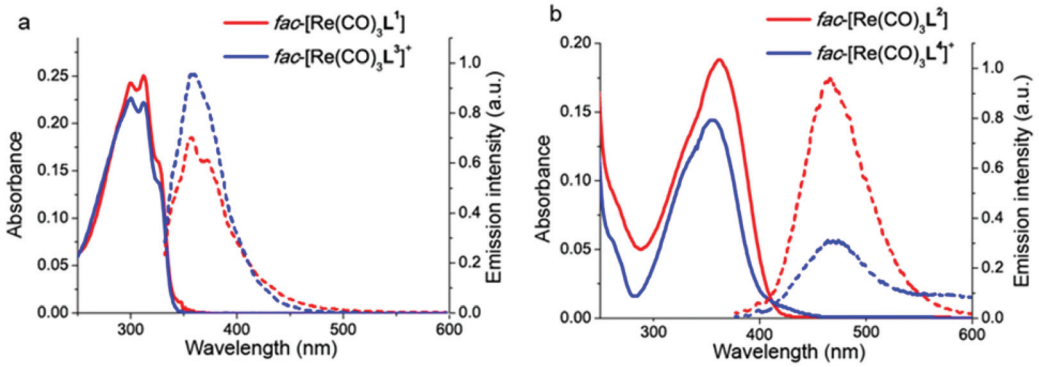

Fig. 6 Absorbance (solid line) and emission (dotted line) spectra of a) *fac*-[$Re^{I}(CO)_3L^1$] (5 μm) and *fac*-[$Re^{I}(CO)_3L^3$]$^+$ (2 μm) in acetonitrile, λ_{ex} = 312 nm, and (b) *fac*-[$Re^{I}(CO)_3L^2$] (5 μM) and *fac*-[$Re^{I}(CO)_3L^4$]$^+$ (5 μM) in acetonitrile, λ_{ex} = 355 nm.

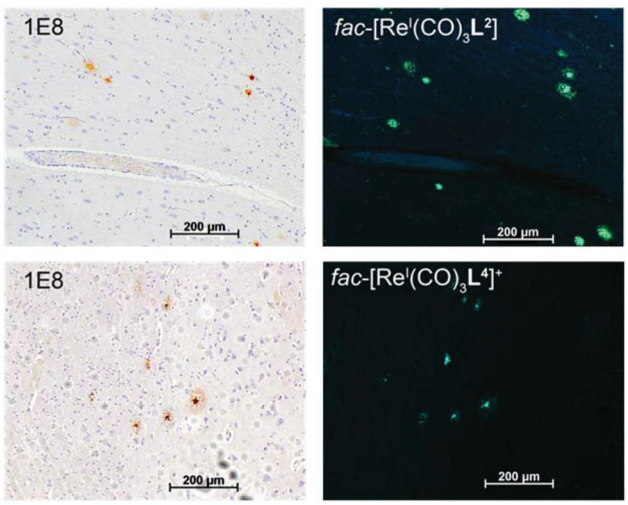

Fig. 7 Tissue sections from the frontal cortex of an AD affected brain (×10 magnification). Images on the left are immunohistologically stained using 1E8 antibody and viewed by bright-field microscopy. The matching adjacent slides treated with the rhenium complex and viewed by epifluorescence microscopy are on the right (λ_{ex} = 359 nm, λ_{em} = 461 nm.

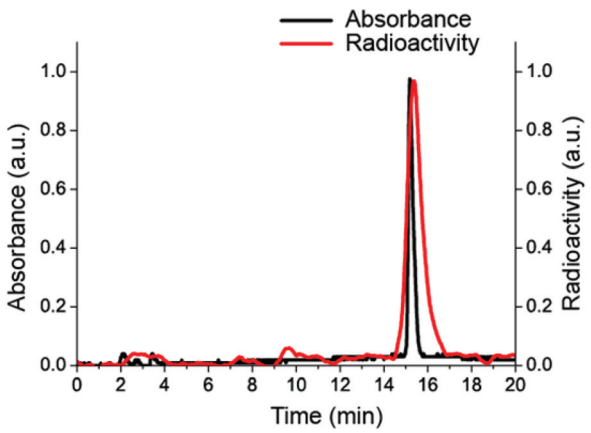

Fig. 8 Representative RP-HPLC trace of (a) *fac*-[$M(CO)_3L^1$] (where M = Re^{I}, black; M = $^{99m}Tc^{I}$, red). Absorbance measured at 254 nm.

1E8 antibody on the adjacent slide (Fig. 7) especially with the plaque cores. Encouragingly there was no evidence of non-specific binding in the tissue from aged matched control subjects after treatment with *fac*-[$Re^{I}(CO)_3L^2$] or *fac*-[$Re^{I}(CO)_3L^4$]$^+$ (see ESI†).

Synthesis of *fac*-[$^{99m}Tc^{I}(CO)_3L^{1-2}$] & *fac*-[$^{99m}Tc^{I}(CO)_3L^{3-4}$]$^+$. Synthesis of technetium complexes, *fac*-[$^{99m}Tc^{I}(CO)_3L^{1-2}$] and *fac*-[$^{99m}Tc^{I}(CO)_3L^{3-4}$]$^+$, involved addition of the tridentate ligands to *fac*-[$^{99m}Tc^{I}(CO)_3(H_2O)$]$^+$, adjustment of the reaction mixture to pH 6 and incubation of the mixture at 70 °C for 20 min. The RP-HPLC profile of the technetium complexes was compared to the respective analogous rhenium complex. The slight difference in the retention times between the UV-Vis detection of the Re complexes and the radioactive peak of the technetium complexes is at least partially attributed to the configuration of the detectors. Both carboxylate containing ligands, HL^1 and HL^2, labelled with high radiochemical yield, affording *fac*-[$^{99m}Tc^{I}(CO)_3L^1$] and *fac*-[$^{99m}Tc^{I}(CO)_3L^2$] in >98% radiochemical purity without purification (Fig. 8). A mixture of products was formed when reacting *fac*-[$^{99m}Tc^{I}(CO)_3(H_2O)$]$^+$ with the ligands containing two pyridyl functional groups, L^3 and L^4. Radiochemical purity of the desired complexes after incubation at 70 °C for 20 min was ~50% and ~40%, for *fac*-[$^{99m}Tc(CO)_3L^3$]$^+$ and *fac*-[$^{99m}Tc(CO)_3L^4$]$^+$ respectively. The complexes were found to be stable over several hours allowing sufficient time for purification by 'Sep-Pak' reverse phase C18 columns. The use of aqueous ethanol improved the radiochemical purity of *fac*-[$^{99m}Tc(CO)_3L^4$]$^+$ to 80%.

The lipophilicity of the complexes was estimated by measuring the partitioning of *fac*-[$^{99m}Tc^{I}(CO)_3L^{1-2}$] and *fac*-[$^{99m}Tc^{I}(CO)_3L^{3-4}$]$^+$ between 1-octanol and PBS (pH 7.4) to give a log $D_{7.4}$ value. It is difficult to predict if small molecules will be capable of crossing the blood-brain barrier but lipophilicity is an important criterion to be considered. Compounds with a log P of 1–3.5 are considered to have the best potential to cross the blood-brain barrier.[37] The log $D_{7.4}$ values ranged from 1.0 for *fac*-[$^{99m}Tc^{I}(CO)_3L^4$]$^+$ to 2.1 for *fac*-[$^{99m}Tc^{I}(CO)_3L^1$]. The addition of the dimethylamino functional group results in complexes that are less lipophilic (Table 2).

Table 2 Log $D_{7.4}$ values of *fac*-[^{99m}Tc^{I}(CO)$_3$**L**$^{1-2}$] and *fac*-[^{99m}Tc^{I}(CO)$_3$**L**$^{3-4}$]$^+$

	fac-[^{99m}Tc^{I}(CO)$_3$**L**^{1}]	*fac*-[^{99m}Tc^{I}(CO)$_3$**L**^{2}]	*fac*-[^{99m}Tc^{I}(CO)$_3$**L**^{3}]$^+$	*fac*-[^{99m}Tc^{I}(CO)$_3$**L**^{4}]$^+$
Log $D_{7.4}$	2.1	1.7	1.8	1.0

Table 3 Biodistribution of *fac*-[^{99m}Tc(CO)$_3$**L**^{2}] in APP/PS1 transgenic mice and wild-type-mice(n = 3); Average %dose/g (standard deviation)

	Wild-type		APP/PS1	
	2 min Ave (std)	30 min Ave (std)	2 min Avg (std)	30 min Avg (std)
Blood	12.87 (3.82)	9.75 (0.43)	11.71 (0.62)	8.47 (1.04)
Brain	0.25 (0.05)	0.21 (0.02)	0.24 (0.02)	0.19 (0.01)
Liver	26.95 (7.84)	26.13 (4.69)	24.64 (5.70)	20.32 (0.65)
Spleen	7.88 (3.80)	8.97 (4.77)	6.67 (1.07)	5.96 (0.97)
Heart	5.43 (1.84)	4.25 (0.62)	5.25 (0.48)	3.59 (0.20)
Stomach	1.69 (0.81)	3.77 (0.70)	2.06 (0.93)	2.19 (1.68)
Kidney	25.32 (9.24)	19.60 (1.09)	24.76 (4.29)	18.45 (0.90)
Intestine	3.15 (0.91)	4.39 (1.71)	3.15 (1.02)	4.15 (0.59)

Stability of *fac*-[^{99m}Tc^{I}(CO)$_3$L**^{2}] & *fac*-[^{99m}Tc^{I}(CO)$_3$**L**^{4}]$^+$ in blood serum and *in vivo* biodistribution.** The complexes *fac*-[Tc^{I}(CO)$_3$**L**^{2}] and *fac*-[Tc^{I}(CO)$_3$**L**^{4}]$^+$ were added to human sera and incubated at 37 °C with aliquots of the mixture taken for analysis by RP-HPLC. Proteins were removed by addition of acetonitrile to incipient precipitation followed by centrifugation and the supernatant was analysed by HPLC. The neutral complex, *fac*-[^{99m}Tc^{I}(CO)$_3$**L**^{1}] remains stable in serum for over three hours but there is some degradation of the cationic complex, *fac*-[^{99m}Tc^{I}(CO)$_3$**L**^{4}]$^+$, evident after incubation in serum but the complex still retained ~60% radiochemical purity.

The biodistribution of *fac*-[^{99m}Tc(CO)$_3$**L**^{2}] was investigated in both wild-type (WT) and 10 month old APP/PS1 transgenic mice. The APP/PS1 transgenic (Tg) amyloid model results in high Aβ plaque levels in the brain. The accumulation of radioactivity was predominately in the liver and kidneys. Brain uptake was detected at 2 min post injection (0.25% ID g^{-1} for WT and 0.24% ID g^{-1} for Tg) but with no statistically significant difference between wild-type and transgenic mice at either 2 minutes or 30 minutes post injection (mpi) (2 mpi, p = 0.429; 30 mpi, p = 0.136) (Table 3). An effective radiotracer for Aβ plaques would record higher radioactivity for brain tissue from the transgenic mice, particularly at 30 min post injection.

Micro-SPECT images of transgenic mice (3 × APP/PS1) were acquired after administering *fac*-[^{99m}Tc^{I}(CO)$_3$**L**^{4}]$^+$ by intravenous tail injection with anatomical information afforded by X-ray computed tomography (CT). Post-mortem immunohistochemical staining of brain tissue samples confirmed the presence of Aβ plaques. Visual inspection of the co-registered SPECT/CT images reveal that activity due to accumulation of ^{99m}Tc is concentrated within the thoracic region with activity also detected in the abdomen and the thyroid (Fig. 9).

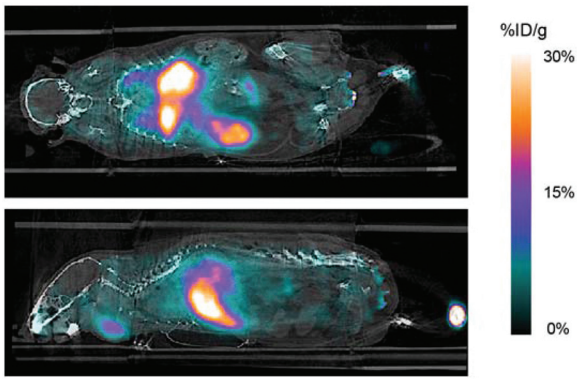

Fig. 9 Coronal and sagittal co-register SPECT/CT images of an APP/PS1 transgenic mouse after intravenous tail injection of *fac*-[^{99m}Tc(CO)$_3$**L**^{4}]$^+$ (~3.5 MBq in 200 μL of 10% ethanol in saline (0.9%)). Amount of radioactivity is shown by the scale bar on the right.

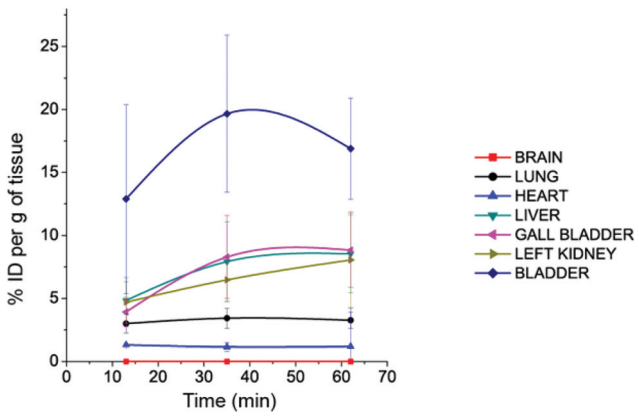

Fig. 10 Time activity plot of selected organs from transgenic mice administered *fac*-[^{99m}Tc(CO)$_3$**L**^{4}]$^+$. Activity was recorded at 13 min, 35 min and 62 min.

Retention of activity within the thyroid may indicate instability of the complex, *fac*-[^{99m}Tc(CO)$_3$**L**^{4}], with respect to oxidation, resulting in formation of pertechnetate ([^{99m}Tc^{VII}O$_4$]$^-$).[38] No uptake is apparent in the cranial region indicating no or very low brain uptake of *fac*-[^{99m}Tc^{I}(CO)$_3$**L**^{4}]$^+$. A plot of activity over time confirms the lack of *fac*-[^{99m}Tc^{I}(CO)$_3$**L**^{4}]$^+$ uptake across the blood-brain barrier *in vivo* (Fig. 10). The majority of activity was shown to be within the bladder. A large amount of activity was also recorded within the gall bladder and liver indicating excretion of the compound by both the urinary and hepatobiliary system.

Conclusion

Four tridentate ligands designed to coordinate to *fac*-$[Re^{I}(CO)_3]^+$ and *fac*-$[^{99m}Tc^{I}(CO)_3]^+$ and bind to Aβ plaques *via* a stilbene functional group were synthesised. The rhenium complexes were characterised by a combination of NMR, electronic spectroscopy and mass spectrometry, and two rhenium complexes were characterised by X-ray crystallography. The complexes with an electron-donating dimethylamino substituent on the stilbene functional group, *fac*-$[Re^{I}(CO)_3\mathbf{L^2}]$ and *fac*-$[Re^{I}(CO)_3\mathbf{L^4}]^+$, bound to Aβ plaques present in post-mortem brain tissue collected from human AD subjects. Analogous technetium complexes were prepared from $[^{99m}Tc^{VII}O_4]^-$ using an 'Isolink' kit that uses potassium boranocarbonate as both a reducing agent and a source of carbon monoxide. The neutral complexes $[^{99m}Tc^{I}(CO)_3\mathbf{L^1}]$ and $[^{99m}Tc^{I}(CO)_3\mathbf{L^2}]$ were more stable in human serum than the cationic complexes, $[^{99m}Tc^{I}(CO)_3\mathbf{L^3}]$ and $[^{99m}Tc^{I}(CO)_3\mathbf{L^4}]$ and all four technetium complexes have log $D_{7.4}$ values that suggested appropriate lipophilicity for penetration of the blood-brain barrier *via* non-facilitated processes. Preliminary biodistribution and micro-SPECT imaging experiments revealed that although neutral $[^{99m}Tc^{I}(CO)_3\mathbf{L^2}]$ displayed higher brain uptake than cationic $[^{99m}Tc^{I}(CO)_3\mathbf{L^4}]$, the degree of brain uptake in a transgenic murine model of amyloid pathology was relatively low (0.24% ID g^{-1}). Effective penetration of the blood-brain barrier is a major challenge in the development of metal-based imaging agents designed to offer insight into the molecular aspects of neurodegeneration. Compounds that bind to Aβ plaques are often lipophilic and consequently display high levels of deposition in the lungs and liver and also susceptible to metabolism by P450 enzymes. Nonspecific binding to albumin and other serum proteins can also decrease the dose of a particular tracer that enters the brain. It would be of interest to investigate if these technetium complexes are substrates for either *p*-glycoprotein or breast cancer resistant protein, as both function as efflux pumps that act to remove substrates from the brain.[39–41] The relative small size and low molecular weight of the $[Tc^{I}(CO)_3]^+$ core makes it attractive for the synthesis of lipophilic and neutral molecules capable of crossing the blood-brain barrier and providing diagnostic information on Aβ plaque burden central to the progression of Alzheimer's disease. In this work tridentate ligands with a stilbene functional group were used to form complexes featuring the $[Re^{I}(CO)_3]^+$ core that bound to Aβ plaques in human subjects. This chemistry was extended to make complexes based on $[^{99m}Tc^{I}(CO)_3]^+$ and further investigations aimed at structural modifications for improving the brain uptake of these complexes is warranted.

Experimental

General synthetic chemistry procedures

All reagents and solvents were obtained from commercial sources and used as received unless otherwise stated. Microwave reactions were carried out using a Biotage Initiator microwave reactor. Nuclear magnetic spectra were acquired on an Agilent 400-MR (^{1}H NMR at 400 MHz and $^{13}C\{^1H\}$ NMR at 101 MHz) or Varian FT-NMR 500 spectrometer (^{1}H NMR at 500 MHz and $^{13}C\{^1H\}$ NMR at 126 MHz) at 298 K. All chemical shifts were referenced to the internal solvent residue and quoted in ppm relative to TMS. Chemical & Micro Analytical Services Pty. Ltd., Victoria, Australia, carried out elemental analyses for C, H and N. Analytical radio-HPLC was performed using a Shimadzu 10AVP UV–Vis detector (Shimadzu, Kyoto, Japan), two LC-10ATVP solvent delivery systems (for solvent A (0.1% trifluoroacetic acid in MilliQ H_2O) & B (0.1% trifluoroacetic acid in acetonitrile)), a Nacalai Tesque Cosmosil 5C18-AR Waters column (4.6 mm I.D. × 150 mm) (Nacalai Tesque, Kyoto, Japan). The mobile phase used was a gradient consisting of 5% solvent B at t = 0 to 100% solvent B after 20 min. All runs were conducted at a constant total flow rate of 1 mL min^{-1} and the absorbance was monitored at λ 254 nm. The Re analogues of ^{99m}Tc complexes were used to confirm synthesis of complexes by comparison of retention times when analysed by RP-HPLC. Absorbance spectra were obtained on a Shimadzu UV-1650PC UV/visible spectrophotometer and emission spectra were obtained on a Varian CARY Eclipse fluorescence spectrometer, with both performed using capped quartz cuvettes. Infrared spectra were recorded using a Perkin-Elmer Spectrum One FTIR spectrometer, with a zinc selenide/diamond universal ATR 60 sampling accessory.

Crystals of compounds were mounted in low temperature oil then flash cooled. Intensity data were collected at 130 K on an X-ray diffractometer with CCD detector using either Cu-Kα (λ = 1.54184 Å) or Mo-Kα (λ = 0.71073 Å) radiation. Data were reduced and corrected for absorption.[42] The structures were solved by direct methods and difference Fourier synthesis using the SHELX[43] suite of programs as implemented within the WINGX[44] software. Thermal ellipsoid plots were generated using ORTEP-3 software. In both structures *fac*-$[Re(CO)_3\mathbf{L^1}]$ and *fac*-$[Re(CO)_3\mathbf{L^3}]CF_3SO_3$ the *trans*-stilbene moiety was disordered with two orientations of the alkene occupying the same site in the crystal. This was refined as a two-site disorder model with occupancies of *ca.* 63 : 37 for *fac*-$[Re(CO)_3\mathbf{L^1}]$ and 73 : 27 for *fac*-$[Re(CO)_3\mathbf{L^3}]CF_3SO_3$, equivalent carbon–carbon bonds were restrained to have the same bond distances, and equivalent carbon atoms restrained to have similar thermal parameters. The triflate counter-ion of *fac*-$[Re(CO)_3\mathbf{L^1}]CF_3SO_3$ was disordered and could not be modelled satisfactorily. The contributions from this counter-ion were removed using the squeeze procedure,[45] which calculated 232 electrons unaccounted for in the void volume of the unit cell. This is reasonably consistent with four triflate anions in the unit cell. *fac*-$[Re^{I}(CO)_3\mathbf{L^1}]$·0.5MeCN: CCDC 1025768. *fac*-$[Re^{I}(CO)_3\mathbf{L^3}]CF_3SO_3$: CCDC 1025769.

(*E*)-4-(4-Bromostyryl)-*N*,*N*-dimethylaniline (2a). Modified from a literature procedure.[46] To a dry round bottom flask was added 4-bromobenzyl bromide (3.57 g, 14.2 mmol) and triethyl phosphite (7.5 mL, 43.1 mmol). The reaction mixture was heated at reflux for 2.5 h then unreacted triethyl phosphite

was removed by evaporation under reduced pressure and the residue was used without further purification. DMF (8 mL), sodium hydride (80% w/w, 1.01 g, 33.7 mmol) and 4-dimethylaminobenzldehyde (2.10 g, 14.1 mmol) were added to the residue and the mixture was stirred at ambient temperature for 12 h. The reaction was quenched by the addition of ethanol then water to afford a green precipitate. The precipitate was collected by filtration, dissolved in dichloromethane (40 mL), washed with water (3 × 40 mL), and the organic phase was then dried ($MgSO_4$). The $MgSO_4$ was removed by filtration and petroleum spirits (boiling range 40–60 °C) were added to the filtrate to give (*E*)-4-(4-bromostyryl)-*N*,*N*-dimethylaniline as yellow plate-like crystals (3.75 g, 12.4 mmol, 88%). ^{1}H NMR (400 MHz; $CDCl_3$): δ 7.43 (m, 4H, Ar*H*), 7.34 (m, AA′BB′, 2H, Ar*H*), 7.03 (d, $^3J_{HH}$ = 16.3, 1H, C*H*═CH), 6.84 (d, $^3J_{HH}$ = 16.3, 1H, CH═C*H*), 6.72 (m, AA′BB′ 2H, Ar*H*), 2.99 (s, 6H, N(CH_3)$_2$). ESI-MS (+ve ion) $[M + H]^+$ *m*/*z* 302.071 (experimental), 302.05 (calculated for $C_{16}H_{17}BrN^+$).

4-(4-Dimethylamino)styryl)benzaldehyde (2). Modified from a literature procedure.[46] To anhydrous and deoxygenated THF (5 mL) was added (*E*)-4-(4-bromostyryl)-*N*,*N*-dimethylaniline (0.48 mg, 1.6 mmol) and the mixture was cooled to −78 °C. To the reaction mixture was added *n*-butyl lithium (1.2 M, 2 mL, 2.4 mmol) dropwise and then DMF (2.6 mL). The mixture was stirred for 3.5 h at −78 °C and then the reaction was diluted with diethyl ether (1 mL) followed by water to afford a bright yellow precipitate. The reaction mixture was extracted with dichloromethane (150 mL), washed with brine (100 mL), then water (3 × 100 mL), the organic phase was then dried ($MgSO_4$), filtered and the solvent removed by evaporation under reduced pressure to afford 4-(4-dimethylamino)styryl)benzaldehyde as an orange crystalline powder (0.32 mg, 1.3 mmol, 82%). ^{1}H NMR (400 MHz; $CDCl_3$): δ 7.43 (m, 4H), 7.33 (d, *J* = 8.4, 2H), 7.03 (d, $^3J_{HH}$ = 16.3, 1H), 6.84 (d, $^3J_{HH}$ = 16.3, 1H), 6.72 (m, 2H), 2.99 (s, 6H). ESI-MS (+ve ion) $[M + H]^+$ *m*/*z* 252.155 (experimental), 252.14 (calculated).

(*E*)-1-(Pyridin-2-yl)-*N*-(4-styrylbenzyl)methanamine (3). To anhydrous ethanol (80 mL) was added 2-picolylamine (1 mL, 9.7 mmol) and *trans*-4-stilbene-carboxyaldehyde (0.98 g, 4.7 mmol). The reaction mixture was heated at reflux under an atmosphere of N_2. After 30 min sodium borohydride (0.71 g, 19 mmol) was added in small portions and the reaction was heated at reflux again. After 6 hours at reflux the reaction was cooled to ambient temperature, the mixture was adjusted to pH 10 (1 M NaOH) then to pH 7 (1 M HCl). The reaction mixture was extracted with dichloromethane and the organic phase was washed (3 × 100 mL, H_2O). The organic phase was dried ($MgSO_4$), filtered, the solvent removed by evaporation under reduced pressure, and the residue was dried under vacuum to yield a colourless wax (1.3 g, 4.4 mmol, 93%). Calc. for $C_{21}H_{20}N_2 \cdot 0.75H_2O$: C, 80.35; H, 6.90; N, 8.98. Found: C, 80.4; H, 6.7; N, 8.9. ^{1}H NMR (500 MHz; $CDCl_3$): δ 8.62 (d, *J* = 4.7, 1H), 7.68 (m, 1H, Py*H*), 7.57–7.52 (m, 4H, Ar*H*), 7.41–7.35 (m, 5H, Ar*H*, Py*H*), 7.30 (m, 1H, Ar*H*), 7.21 (m, 1H, Py*H*), 7.15 (s, 2H, C*H*═C*H*), 3.99 (s, 2H, CH_2), 3.90 (s, 2H, CH_2), 2.27 (s, 1H, N*H*). $\{^1H\}^{13}$C NMR (126 MHz; $CDCl_3$): δ 159.8, 149.4, 139.83, 137.5, 136.5, 136.2, 128.8, 128.7, 128.6, 128.4, 127.6, 126.7, 126.6, 122.5, 122.0, 54.6, 53.3. ESI-MS (+ve ion) *m*/*z* $[M + H]^+$ 301.170 (experimental), 301.17 (calculated for $C_{21}H_{21}N_2^+$).

(*E*)-*N*,*N*-Dimethyl-4-(4-((pyridin-2-ylmethylamino)methyl)-styryl)aniline (4). To anhydrous ethanol (50 mL) was added 2-picolylamine (0.44 g, 9.7 mmol) and **2** (0.36 g, 1.4 mmol). The reaction mixture was set stirring and heated at reflux. After 1 h, sodium borohydride (0.70 g, 18.5 mmol) was added in small portions and the reaction was heated at reflux again. After 6 hours, the reaction was cooled to ambient temperature and the mixture was adjusted to pH 12 (1 M NaOH) and then pH 7 (1 M HCl). After extracting the reaction mixture with ethyl acetate the organic layer was washed with brine (2 × 100 mL), and then with water (3 × 100 mL), dried over $MgSO_4$, filtered and the solvent was evaporated under reduced pressure. The resultant waxy yellow residue was triturated with petroleum benzene (boiling range 40–60%) and isolated by filtration followed by purification by silica chromatography (chloroform) to afford compound **4** as a yellow powder (0.33 g, 0.97 mmol, 68%). Calc. for $C_{23}H_{25}N_3 \cdot 0.5H_2O$: C, 78.37; H, 7.44; N, 11.92. Found: C, 78.7; H, 7.30; N, 12.10. ^{1}H NMR (500 MHz; $CDCl_3$): δ 8.57 (m, 1H, py*H*), 7.64 (m, 1H, Py*H*), 7.45–7.40 (m, 5H), 7.32 (m, 3H, Py*H*, Ar*H*), 7.17–7.15 (m, 1H, Py*H*), 7.03 (d, $^3J_{HH}$ = 16.2, 1H, CH═C*H*), 6.91 (d, $^3J_{HH}$ = 16.3, 1H, C*H*═CH), 6.72 (m, 2H, Ar*H*), 3.94 (s, 2H, CH_2), 3.84 (s, 2H, CH_2), 2.98 (s, 6H, N(CH_3)$_2$). $\{^1H\}^{13}$C NMR (126 MHz; $CDCl_3$): δ 160.0, 150.2, 149.5, 138.8, 137.2, 136.5, 128.7, 128.6, 127.7, 126.2, 126.0, 124.4, 122.5, 122.0, 112.6, 54.7, 53.4, 40.6. ESI-MS (+ve ion) $[M + Na]^+$ *m*/*z* 344.212, (experimental), 344.21 (calculated for $C_{23}H_{26}N_3^+$).

(*E*)-Methyl 3-((pyridin-2-ylmethyl)(4-styrylbenzyl)amino)propanoate (methyl ester of L^1). To ethanol (30 mL) was added **3** (0.40 g, 1.3 mmol), methyl acrylate (0.25 mL, 2.8 mmol) and acetic acid (0.20 mL, 3.5 mmol). The mixture was heated at reflux for 26 h then cooled to ambient temperature and the solvent was removed by evaporation under reduced pressure. The crude product was eluted through a plug of silica using ethyl acetate, the solvent removed and the residue dried *in vacuo* to afford the methyl ester of **L^1** as a yellow oil (0.32 g, 0.83 mmol, 62%). Calc. for $C_{25}H_{26}N_2O_2$: C, 77.69; H, 6.78; N, 7.25. Found: C, 77.5; H, 6.7; N, 7.2. ^{1}H NMR (500 MHz; $CDCl_3$): δ 8.51 (ddd, $^3J_{HH}$ = 4.9, $^4J_{HH}$ = 1.8, $^5J_{HH}$ 0.9 Hz, 1H, Py*H*), 7.66 (m, 1H, Py*H*), 7.52–7.49 (m, 3H, Ar*H*), 7.47–7.45 (m, 2H, Ar*H*), 7.37–7.32 (m, 4H, Ar*H*), 7.25 (m, 1H, Py*H*), 7.15 (ddd, $^3J_{HH}$ = 7.4, $^3J_{HH}$ = 4.9, $^3J_{HH}$ = 1.2 Hz, 1H, Py*H*), 7.09 (s, 2H, C*H*═C*H*), 3.77 (s, 2H, CH_2), 3.65 (s, 2H, CH_2), 3.63 (s, 3H, CH_3), 2.88 (t, $^3J_{HH}$ = 7.1 Hz, 2H, CH_2–CH$_2$), 2.54 (t, $^3J_{HH}$ = 7.1 Hz, 2H, CH$_2$–CH_2). $\{^1H\}^{13}$C (126 MHz; $CDCl_3$): δ 173.0, 159.9, 149.0, 138.6, 137.5, 136.5, 136.4, 129.3, 128.8, 128.6, 128.5, 127.7, 126.6, 126.6, 123.0, 122.1, 60.0, 58.3, 51.6, 49.7, 32.8. ESI-MS (+ve ion) *m*/*z* $[M + H]^+$ 387.211 (experimental), 387.21 (calculated for $C_{25}H_{26}N_2O_2^+$).

(*E*)-Methyl 3-((4-(4-(dimethylamino)styryl)benzyl)(pyridine-2-ylmethyl)amino)propanoate (methyl ester of L^2). To ethanol (10 mL) was added **4** (0.40 g, 1.3 mmol), methyl acrylate

(0.25 mL, 2.8 mmol) and acetic acid (0.20 mL, 3.5 mmol). The reaction mixture was shielded from light and stirred at ambient temperature under nitrogen atmosphere. After 48 h, the solvent and unreacted methyl acrylate were removed *in vacuo* to afford the methyl ester of $\mathbf{L^2}$ as a yellow oil. (0.32 g, 0.74 mmol, 98%). ^{1}H NMR (400 MHz; $CDCl_3$): δ 8.50 (m, 1H, Py*H*), 7.65 (m, 1H, Py*H*), 7.49 (d, $^3J_{HH}$ = 7.9, 1H, Py*H*), 7.43–7.39 (m, 4H, Ar*H*), 7.29 (m, AA′BB′, 2H, Ar*H*), 7.14 (ddd, $^3J_{HH}$ = 7.4, $^3J_{HH}$ = 4.9, $^4J_{HH}$ = 1.0, 1H, Py*H*), 7.02 (d, $^3J_{HH}$ = 16.3, 1H, C*H*═CH), 6.89 (d, $^3J_{HH}$ = 16.3, 1H, CH═C*H*), 6.71 (m, AA′BB′, 2H, Ar*H*), 3.76 (s, 2H, CH_2), 3.62 (s, 2H), 2.98 (s, 6H, N(CH_3)$_2$), 2.87 (t, $^3J_{HH}$ = 7.1, 2H, CH_2), 2.53 (t, $^3J_{HH}$ = 7.1, 2H, CH_2). ESI-MS (+ve ion) $[M + H]^+$ *m*/*z* 430.259 (experimental), 430.25 (calculated for $C_{27}H_{32}N_3O_2^+$).

(*E*)-3-((4-(4-(Dimethylamino)styryl)benzyl) (pyridine-2-ylmethyl)amino)propanoic acid ($\mathbf{HL^2}$). To a mixture of methanol and distilled water (1 : 1, 14 mL) was added the methyl ester of $\mathbf{L^2}$ (0.25 g, 0.58 mmol), $CsCO_3$ (.40 g, 1.1 mmol) and the reaction mixture was set stirring and heated at reflux for 1 h. The reaction mixture was then extracted into dichloromethane by gradual addition of HCl to the aqueous layer. The organic phase was dried ($MgSO_4$) and the solvent removed by evaporation under reduced pressure to afford $\mathbf{HL^2}$ as a light yellow powder (0.16 g, 0.39 mmol, 67%). Calc. for $C_{26}H_{29}N_3O_2{\cdot}H_2O$: C, 72.03; H, 7.21; N, 9.69. Found: C, 72.0; H, 6.8; N, 9.7. ^{1}H NMR (500 MHz; $CDCl_3$): δ 8.59 (m, 1H, Py*H*), 7.67 (m, 1H, Py*H*), 7.43 (m, 4H, Ar*H*), 7.26 (m, AA′BB′, 2H, Ar*H*), 7.23 (m, 2H, Py*H*), 7.04 (d, $^3J_{HH}$ = 16.3, 1H, CH_2═CH$_2$), 6.88 (d, $^3J_{HH}$ = 16.3, 1H, CH$_2$═CH_2), 6.71 (m, AA′BB′, 2H, Ar*H*), 3.85 (s, 2H, CH_2), 3.78 (s, 2H, CH_2), 2.97 (m, 8H, CH_2, N(CH_3)$_2$), 2.58 (t, $^3J_{HH}$ = 6.2, 2H, CH_2). ^{13}C NMR (126 MHz; $CDCl_3$): δ 173.6, 156.5, 150.3, 149.3, 138.2, 137.2, 133.9, 130.0, 129.4, 127.8, 126.4, 125.7, 123.8, 123.7, 122.9, 58.1, 57.8, 49.3, 40.6, 31.1. ESI-MS (+ve ion) $[M + H]^+$ *m*/*z* 416.234 (experimental), 416.23 (calculated for $C_{26}H_{30}N_3O_2^+$).

(*E*)-2-(Pyridin-2-yl)-*N*-(pyridin-2-ylmethyl)-*N*-(4-styrylbenzyl)-ethanamine ($\mathbf{L^3}$). To ethanol (40 mL) was added 2-vinylpyridine (0.35 mL, 3.2 mmol), **3** (0.48 g, 1.6 mmol) and acetic acid (0.40 mL, 7.0 mmol). The reaction mixture was heated at reflux for 36 h. The crude product was loaded onto a plug of silica and washed with 10% ethyl acetate in dichloromethane, 10% MeOH in ethyl acetate then eluted using 15% MeOH in ethyl acetate. The solvent was removed by evaporation under reduced pressure and the residue dried to afford $\mathbf{L^3}$ as a colourless wax (within crude: 0.39 g, 0.96 mmol, 99%). Calc. for $C_{20}H_{17}N_3{\cdot}0.5H_2O$: C, 77.90; H, 5.88; N, 13.63. Found: C, 77.5; H, 5.8; N, 13.9.^{1}H NMR (500 MHz; $CDCl_3$): δ 8.49 (m, 2H, Py*H*), 7.57 (m, 2H, Py*H*), 7.50 (m, 2H, Ar*H*), 7.42 (m, AA′BB′, 2H), 7.36 (m, 3H), 7.28 (m, AA′BB′, 2H), 7.27 (m, 1H, Py*H*), 7.10 (m, 5H,Py*H*, C*H*═C*H*), 3.82 (s, 2H, CH_2), 3.71 (s, 2H,CH_2), 3.04 (m, 2H, CH_2–CH$_2$), 2.95 (m, 2H, CH$_2$–CH_2). $\{^1H\}^{13}$C NMR (126 MHz; $CDCl_3$): δ 160.5, 159.9, 149.1, 148.8, 138.7, 137.5, 136.6, 136.4, 129.3, 128.8, 128.8, 128.6, 128.5, 127.7, 126.6, 126.5, 123.6, 123.0, 122.1, 121.3, 59.9, 58.4, 54.1, 359. ESI-MS (+ve ion) *m*/*z* $[M + H]^+$ 406.228 (experimental), 406.23 (calculated for $C_{28}H_{28}N_3^+$).

(*E*)-*N*,*N*-Dimethyl-4-(4-(((2-(pyridin-2-yl)ethyl)(pyridin-2-ylmethyl)amino)methyl)styryl)aniline ($\mathbf{L^4}$). To ethanol (10 mL) was added **4** (0.31 g, 0.90 mmol), 2-vinylpyridine (0.25 mL, 2.3 mmol) and acetic acid (0.25 mL, 4.4 mmol). The reaction mixture was shielded from light and stirred at ambient temperature under nitrogen atmosphere for 11 days, the solvent and excess 2-vinylpyridine were removed under reduced pressure to afford $\mathbf{L^4}$ as a yellow oil, (0.38 g, 0.74 mmol, 97%), which was purified by silica chromatography ($CHCl_3$–CH_3OH). Calc. for $C_{30}H_{32}N_4{\cdot}0.5H_2O$: C, 78.74; H, 7.37; N, 12.24. Found: C, 79.0; H, 7.3; N, 12.2. ^{1}H NMR (500 MHz; $CDCl_3$): δ 8.48 (m, 2H, Py*H*), 7.56 (m, 2H, Py*H*), 7.42–7.38 (m, 4H, Ar*H*), 7.36 (m, 2H, Py*H*), 7.25 (m, AA′BB′, 2H, Ar*H*), 7.09 (m, 2H, Py*H*), 7.01 (d, $^3J_{HH}$ = 16.3, 1H), 6.89 (d, $^3J_{HH}$ = 16.3, 1H), 6.70 (m, AA′BB′, 2H), 3.82 (s, 2H, CH_2), 3.70 (s, 2H, CH_2), 2.98 (m, 10H, CH_2–CH_2, N(CH_3)$_2$). $\{^1H\}^{13}$C NMR (126 MHz; $CDCl_3$): δ 160.8, 160.4, 150.2, 149.3, 148.9, 138.0, 137.0, 136.4), 136.2, 129.2, 128.5, 127.6, 126.0, 126.0, 124.4, 123.5, 122.9, 121.9, 121.2, 112.6, 60.2, 58.4, 54.2, 40.6, 36.2. ESI-MS (+ve ion) $[M + H]^+$ *m*/*z* 449.283 (experimental), 449.27 (Calculated).

***fac*-$[Re^I(CO)_3L^1]$.** To aqueous NaOH (1 M, 3 mL) was added the methyl ester of $\mathbf{L^1}$ (40 mg, 0.10 mmol). The reaction mixture was heated at reflux for 30 min then the mixture was allowed to cool to ambient and transferred to a microwave reaction flask. Methanol (7 mL) and $[Re^I(CO)_5OTf]$ (51 mg, 0.11 mmol) were added and the pH adjusted to ~pH 7 by addition of HCl (1 M). The flask was capped and irradiated at 150 °C (3 × 10 min) shaking between each heating cycle. The solvent volume was reduced by evaporation under a stream of nitrogen until the point of turbidity. The flask was sealed and stored at 4 °C for 2 days and colourless crystals were observed. The solvent was decanted and the crystals washed with H_2O and dried *in vacuo* to afford *fac*-$[Re^I(CO)_3L^1]$ as a colourless crystalline powder (40 mg, 0.062 mmol, 57%). Calc. for $C_{27}H_{23}N_2O_5Re$: C, 50.54; H, 3.61; N, 4.37. Found: C, 50.52; H, 3.67; N, 4.30. IR (thin film) ν(CO) 2017 cm^{-1}, 1903 cm^{-1}, 1873 cm^{-1}. ^{1}H NMR (500 MHz; $CDCl_3$): δ 8.92 (m, 1H, Py*H*), 7.93 (m, 1H, Py*H*), 7.62 (m, AA′BB′, 2H, Ar*H*), 7.54 (m, AA′BB′, 2H, Ar*H*), 7.47 (m, 1H, Py*H*), 7.39 (m, 3H, Py*H*, Ar*H*), 7.32 (m, 3H, Ar*H*), 7.20 (d, $^3J_{HH}$ = 16.4 Hz, 1H, C*H*═CH), 7.13 (d, $^3J_{HH}$ = 16.3 Hz, 1H, CH═C*H*), 4.88 (m, AB, 1H, CH_2), 4.65 (m, AB, 1H, CH_2), 4.56 (m, AB, 1H, CH_2), 4.02 (m, AB, 1H, CH_2), 2.92 (m, 1H,CH_2–CH$_2$), 2.82 (m, 1H, CH$_2$–CH_2), 2.41 (m, 1H, CH$_2$–CH_2), 2.23 (m, 1H, CH_2–CH$_2$). $\{^1H\}^{13}$C NMR (126 MHz; $CDCl_3$): δ 197.2, 195.9, 194.1, 177.2, 158.7, 153.8, 139.8, 139.2, 136.8, 132.5, 130.9, 129.5, 129.0, 128.4, 127.3, 127.1, 126.9, 126.2, 123.2, 66.9, 66.0, 49.8, 33.5. ESI-MS (+ve ion) $[M + H]^+$ *m*/*z* 643.108 (experimental), 643.12 (calculated for $C_{27}H_{24}N_2O_5Re^+$). Crystals suitable for X-ray diffraction were grown by evaporation of a solution of the complex dissolved in acetonitrile.

***fac*-$[Re^I(CO)_3L^2]$.** To a microwave reaction flask equipped with a stirrer bar was added $[Re^I(CO)_5OTf]$ (41 mg, 0.10 mmol), and methanol (2.5 mL). The reaction flask was sealed and the mixture was heated to 150 °C using MW irradiation (2 × 15 min). $\mathbf{L^2}$ (42 mg, 0.10 mmol) was added to the reaction mixture and the MW vessel was sealed and

irradiated to 150 °C (15 min) then at 130 °C (10 min). A precipitate was formed upon reducing the solvent volume under a stream of nitrogen. The precipitate was isolated by filtration to afford *fac*-[$Re^{I}(CO)_3\mathbf{L}^2$] as a yellow powder (30 mg, 0.44 mmol, 44%). IR ν(CO) 2021 cm^{-1}, 1906 cm^{-1}, 1886 cm^{-1}. Calc. for $C_{29}H_{28}N_3O_5Re{\cdot}2.5H_2O$: C, 47.73; H, 4.56; N, 5.76. Found: C, 47.8; H, 4.5; N, 5.7. ^{1}H NMR (500 MHz; $CDCl_3$): δ 8.93 (m, 1H, Py*H*), 7.92 (m, 1H, Py*H*), 7.56 (m, AA′BB′, 2H, Ar*H*), 7.43 (m, 4H, Ar*H*, Py*H*), 7.29 (m, AA′BB′, 2H, Ar*H*), 7.13 (d, $^3J_{HH}$ = 16.3, 1H, C*H*═CH), 6.92 (d, $^3J_{HH}$ = 16.3, 1H, CH═C*H*), 6.74–6.72 (m, AA′BB′,2H, Py*H*), 4.87 (m, AB, 1H, CH_2), 4.63 (m, AB, 1H, CH_2), 4.54 (m, AB, 1H, CH*H*), 4.01 (m, AB, 1H, C*H*H), 3.01 (s, 6H, N(CH_3)$_2$), 2.93 (m, 1H, C*H*H–CH_2), 2.82 (m, 1H, CH_2–C*H*H), 2.37 (m, 1H, CH_2–CH*H*), 2.22 (m, 1H, CH*H*–CH_2). {^{1}H}^{13}C NMR (126 MHz; $CDCl_3$): δ 197.2, 195.9, 194.2, 177.3, 158.8, 153.7, 150.7, 140.1, 139.7, 132.4, 131.0, 128.3, 128.0, 126.5, 126.1, 125.1, 123.2, 122.7, 112.5, 66.9, 66.0, 49.7, 40.5, 33.5. ESI-MS(+ve ion) [M + H]$^+$ *m*/*z* 686.164 (experimental), 686.17 (calculated for $C_{29}H_{29}N_3O_5Re$).

***fac*-[$Re^{I}(CO)_3\mathbf{L}^3$]CF_3SO_3.** A microwave reaction flask was charged with $\mathbf{L}^3$ (50 mg, 0.11 mmol), [$Re^{I}(CO)_5OTf$] (43 mg, 1.1 mmol) and methanol (3 mL). The flask was capped and the reaction mixture was irradiated at 150 °C (3 × 10 min), shaking between each heating cycle. To the mixture was added diethyl ether and colourless crystals were observed. The reaction mixture was stored at −18 °C overnight and the resultant crystals were isolated by filtration to afford *fac*-[$Re^{I}(CO)_3\mathbf{L}^3$]-CF_3SO_3 as colourless crystals (63 mg, 0.074 mmol, 70%). Calc. for $C_{32}H_{27}F_3N_3O_6ReSN_3{\cdot}H_2O$: C, 45.60; H, 3.47; N, 4.99. Found: C, 45.7; H, 3.3; N, 4.6. IR ν(CO) 2027 cm^{-1}, 1901 cm^{-1}, 1869 cm^{-1}. ^{1}H-NMR (500 MHz; $CDCl_3$): δ 9.03 (m, 1H, py*H*), 8.92 (m, 1H, Py*H*), 7.93 (m, 1H, Py*H*), 7.86 (m, 1H, Py*H*), 7.67 (m, 3H, Py*H*, Ar*H*), 7.52 (m, 4H, Ar*H*, Py*H*), 7.45 (m, 2H, Ar*H*), 7.39 (m, 3H, Ar*H*, Py*H*), 7.30 (m, 1H, Py*H*), 7.20 (d, $^3J_{HH}$ = 16.4 Hz, 1H, C*H*═CH), 7.13 (d, $^3J_{HH}$ = 16.3 Hz, 1H, CH═C*H*), 4.86 (m, AB, 1H, C*H*H), 4.71 (m, AB, 1H, CH*H*), 4.57 (m, AB, 1H, C*H*H), 4.43 (m, AB, 1H, CH*H*), 3.31 (m, 3H, CH_2–C*H*H), 2.19 (m, 1H, CH_2–CH*H*). {^{1}H}^{13}C NMR (126 MHz; CD_3OD): δ 196.8, 194.9, 194.5, 164.4, 161.5, 156.6, 153.4, 142.0, 141.8, 140.5, 138.4, 134.0, 131.5, 131.2, 129.8, 129.1, 128.5, 128.0, 127.9, 127.7, 127.6, 126.2, 125.7, 121.8 (q), 68.1, 67.9, 51.8, 35.6. ESI-MS (+ve ion) *m*/*z* [M]$^+$ 676.159 (experimental), 676.16 (calculated). Crystals suitable for X-ray diffraction were grown by exchange of vapours between *n*-pentane and a solution of the complex in dichloromethane.

***fac*-[$Re^{I}(CO)_3\mathbf{L}^4$]CF_3SO_3.** To a microwave reaction flask equipped with a stirrer bar was added [$Re^{I}(CO)_5OTf$] (40 mg, 0.080 mmol), $\mathbf{L}^4$ (40 mg, 0.090 mmol), and methanol (5 mL). The reaction vessel was sealed and the mixture was heated to 130 °C using microwave irradiation (15 min) followed by further irradiation to 140 °C (15 min). The solvent volume was reduced under a stream of nitrogen and diethyl ether (5 mL) was added, and the mixture was stored at −18 °C for 12 h. The precipitate that formed was collected by filtration to afford *fac*-[$Re^{I}(CO)_3\mathbf{L}^4$]CF_3SO_3 as a yellow powder (15 mg,0.017 mmol, 21%). Calc. for $C_{34}H_{32}N_4F_3O_6ReS$: C, 47.05; H, 3.72; N, 6.46. Found: C, 47.4; H, 3.7; N, 6.4. IR ν(CO) 2020 cm^{-1}, 1903 cm^{-1}, 1882 cm^{-1}. ^{1}H NMR (500 MHz; $CDCl_3$): δ 9.04 (m, 1H, Py*H*), 8.91 (m, 1H, PyH), 7.96 (m, 1H, Py*H*), 7.87 (m, 1H, Py*H*), 7.65 (m, 1H, Py*H*), 7.59 (m, AA′BB′, 2H, Ar*H*), 7.52 (m, 2H, Py*H*), 7.43 (m, 5H, Ar*H*, Py*H*), 7.12 (d, $^3J_{HH}$ = 16.2 Hz, 1H, C*H*═CH), 6.92 (d, $^3J_{HH}$ = 16.3 Hz, 1H, CH═C*H*), 6.75 (m, AA′BB′, 2H, Ar*H*), 4.84 (m, AB, 1H, CH*H*), 4.69 (m, AB, 1H, C*H*H), 4.55 (m, AB, 1H, CH*H*), 4.38 (m, AB, 1H, C*H*H), 3.29 (m, 3H, CH_2–C*H*H), 3.01 (s, 6H, N(CH_3)$_2$), 2.19 (m, 1H, CH_2–CH*H*). {^{1}H}^{13}C NMR (126 MHz; $CDCl_3$): δ 195.8, 193.7, 193.5, 162.4, 159.4, 154.9, 151.8, 150.4, 141.3, 140.7, 140.4, 132.6, 131.0, 128.1, 127.9, 127.5, 127.0, 126.8, 125.5, 125.2, 123.0, 112.7, 67.7, 66.9, 51.3, 40.7, 34.8. ESI-MS (+ve ion) [M]$^+$ *m*/*z* 719.199 (experimental), 719.20 (calculated for $C_{33}H_{33}N_4O_3Re^+$).

Staining of human brain tissue

The Health Sciences Human Ethics Sub-committee, The University of Melbourne, approved all experiments using human brain tissue (Ethics Approval No. 1341145). Brain tissue was collected at autopsy. Brain tissue from the frontal cortex was preserved by formalin fixation and paraffin embedding. AD pathology was confirmed according to standard National Institute of Aging and Reagan Institute Working Group on Diagnostic Criteria for the Neuropathological Assessment of Alzheimer's Disease (1997) criteria. The brain tissue samples of age-matched Human control (HC) were subject to the above criteria. Deparaffinization of AD and HC sections (5 μm) was carried out (xylene, 3 × 2 min) prior to rehydration (soaked for 2 min in 100%, 90%, 70%, then 0% ethanol–water v/v). The slides were then washed in PBS (5 min) and the autofluorescence was quenched with potassium permanganate (0.25% in PBS, 20 min) before washing again with PBS (2 × 20 min). Samples were then treated with a solution of potassium metabisulfite and oxalic acid (1% each in PBS) until the tissue changed from brown in colour to colourless then washed in PBS (3 × 2 min). The sections were blocked with bovine serum albumin (2% BSA in PBS, pH 7.4, 10 min) then treated covered with filtered compound (50 μM, 15% DMSO–PBS, 60 min). The sections were treated with BSA to remove any non-specifically bound complex and washed in PBS (3 × 2 min), then distilled water and finally mounted with non-fluorescent mounting media (Dako). Images were obtained on a Leica (Bannockburn, IL) DM1RB microscope fitted with a Carl Zeiss AxioCam MR colour camera.

Radiochemistry

General synthesis of [$^{99m}Tc^{I}(CO)_3\mathbf{L}^{1-4}$] complexes. The *fac*-[$^{99m}Tc^{I}(CO)_3(H_2O)$]$^+$ starting material was prepared as directed by the manufacturer instructions supplied with the Isolink™ kit (Covidien). In short, [$Tc^{VII}O_4$]$^-$ (1000 MBq, in 0.9% saline solution (1 mL)) eluted from a Gentech® generator was added to an Isolink™ kit (Mallinckrodt Medical B.V., The Netherlands) and was heated in a bath of boiling water. After 20 min, the kit was removed from the bath, let cool to ambient temperature and aliquots from the kit, containing *fac*-[$^{99m}Tc^{I}(CO)_3(H_2O)_3$]$^+$, was used for subsequent ^{99m}Tc labelling

of ligands. The radiolabeling of ligands was carried out by addition of *fac*-$[^{99m}Tc^{I}(CO)_3(H_2O)_3]^+$ (100 μL) to a solution of the chosen ligand in dimethyl sulfoxide or ethanol (100 μL, 1 mg mL^{-1}). The reaction mixture was then adjusted to pH 6 by addition of 1 M HCl and incubated at 70 °C for 20 min.

Measurement of Log $D_{7.4}$ values. To a vial containing 1-octanol (5 mL) and PBS (5 mL, 20 mM, pH 7.4) was added the radiotracer (50 μL). The mixture was shaken by hand for 3 min and the fractions were allowed to seperate. The 1-octanol layer used in the subsequent steps and each measurement was carried out in triplicate. An aliquot of the 1-octanol layer (900 μL) was added to PBS (900 μL, 20 mM, pH 7.4). The two phases were mixed by mechanical shaking (5 min) then separated by centrifuge (5 min at 13 200 rpm, Eppendorf 5415 D centrifuge). A 500 μL aliquot of the organic phase and 500 μL from the aqueous phase was taken. The radioactive decay of each aliquot was measured in counts per minute (cpm) (Perkin-Elmer, Wizard 1470 automatic gamma counter) enabling calculation of the partition coefficient (D) and $\log D_{7.4}$.

***In vivo* biodistribution of *fac*-$[^{99m}Tc^{I}(CO)_3L^2]$ in mice.** All methods conformed to the Australian National Health and Medical Research Council published code of practice for animal research and The Howard Florey Animal Ethics Committee approved experimentation. All mice were housed according to standard animal care protocols and fed standard laboratory chow and tap water *ad libitum*. Mice were kept on a 12 : 12 hour light dark cycle and all testing was performed during the light phase of the circadian cycle. All studies were conducted in a blinded fashion.

A DMSO–saline solution (4.8% DMSO, 100 μL volume per dose) of $[^{99m}Tc^{I}(CO)_3\mathbf{L^2}]$ (57 kBq) was injected directly into the tail vein of wild type and APP/PS1 transgenic mice. The mice were euthanized at either 2 or 30 min by intraperitoneal injection of sodium pentobarbitone (80 mg per kg) followed by perfusion with PBS and collection of the brain and other organs. The organs of interest were removed, weighed and the radioactive decay was measured in cpm (Packard Cobra II automatic gamma counter). The percentage dose per organ was calculated by comparison of the tissue counts with aliquots of the injected material.

SPECT/CT imaging of APP/PS1 transgenic mice after injection of *fac*-$[^{99m}Tc^{I}(CO)_3L^4]^+$. To an Isolink™ kit (Mallinckrodt Medical B.V., The Netherlands) was added pertechnetate (1200 MBq in 1 mL 0.9% saline) and the mixture was heated at 100 °C (20 min) affording *fac*-$[^{99m}Tc^{I}(CO)_3(H_2O)_3]^+$. To an Eppendorf™ tube was added $\mathbf{L^4}$ (150 μL of $\mathbf{L^4}$ in ethanol, 1 mg mL^{-1}), saline (0.9%, 352 μL), 1 M HCl (10 μL) and *fac*-$[^{99m}Tc^{I}(CO)_3(H_2O)_3]^+$ (58 μL) and the mixture was heated at 70 °C for 10 min affording *fac*-$[^{99m}Tc^{I}(CO)_3\mathbf{L^4}]^+$. Saline (0.9%, 1140 μL) was added to reduce the concentration of ethanol in the reaction mixture to 10%.

The radiotracer, *fac*-$[^{99m}Tc(CO)_3\mathbf{L^4}]^+$, was administered to APP/PS1 transgenic mice (×3, 15 months old, ~40 g) by intravenous tail injection (200 μL, 10% ethanol, specific activity 168 GBq $mmol^{-1}$). Acquisition of images using a SPECT/CT scanner (Mediso nanoScan SPECT/CT) was accomplished by 3 × 10 min static SPECT scans at approximately 2, 25 and 50 min post injection with one CT scan (25 kVp, 0.45 s, 0.99 mA, helical scan with 720 projections). To confirm the presence of Aβ plaques, brain tissue samples were immunohistochemically stained *ex vivo*, using 1E8 antibody.

Acknowledgements

The Australian Research Council is acknowledged for financial support. Covidien Ltd. provided the 'Isolink' kits used in this research. Dr Nouria Salehi (Royal Melbourne Hospital, Melbourne, Australia) is acknowledged for assistance in analysing biodistribution data. The Victorian Brain Bank is acknowledged for the provision of the brain tissue used in this study.

Notes and references

1 C. L. Masters, G. Simms, N. A. Weinman, G. Multhaup, B. L. McDonald and K. Beyreuther, *Proc. Natl. Acad. Sci. U. S. A.*, 1985, **82**, 4245.
2 J. A. Hardy and G. A. Higgins, *Science*, 1992, **256**, 184.
3 H. F. Kung, S. R. Choi, W. Qu, W. Zhang and D. Skovronsky, *J. Med. Chem.*, 2010, **53**, 933.
4 E. Karran, M. Mercken and B. De Strooper, *Nat. Rev. Drug Discovery*, 2011, **10**, 698.
5 C. C. Rowe and V. L. Villemagne, *J. Nucl. Med.*, 2011, **52**, 1733.
6 C. A. Mathis, Y. Wang, D. P. Holt, G.-F. Huang, M. L. Debnath and W. E. Klunk, *J. Med. Chem.*, 2003, **46**, 2740.
7 W. Zhang, S. Oya, M.-P. Kung, C. Hou, D. L. Maier and H. F. Kung, *Nucl. Med. Biol.*, 2005, **32**, 799.
8 R. Vandenberghe, K. Van Laere, A. Ivanoiu, E. Salmon, C. Bastin, E. Triau, S. Hasselbalch, I. Law, A. Andersen, A. Korner, L. Minthon, G. Garraux, N. Nelissen, G. Bormans, C. Buckley, R. Owenius, L. Thurfjell, G. Farrar and J. Brooks David, *Ann. Neurol.*, 2010, **68**, 319.
9 H. F. Kung, C.-W. Lee, Z.-P. Zhuang, M.-P. Kung, C. Hou and K. Ploessl, *J. Am. Chem. Soc.*, 2001, **123**, 12740.
10 M. Ono, A. Wilson, J. Nobrega, D. Westaway, P. Verhoeff, Z.-P. Zhuang, M.-P. Kung and H. F. Kung, *Nucl. Med. Biol.*, 2003, **30**, 565.
11 P. L. G. Verhoeff Nicolaas, A. Wilson Alan, S. Takeshita, L. Trop, D. Hussey, K. Singh, F. Kung Hank, M.-P. Kung and S. Houle, *Am. J. Geriatr. Psychiatry*, 2004, **12**, 584.
12 W. Zhang, S. Oya, M.-P. Kung, C. Hou, D. L. Maier and H. F. Kung, *J. Med. Chem.*, 2005, **48**, 5980.
13 W. Qu, M.-P. Kung, C. Hou, T. E. Benedum and H. F. Kung, *J. Med. Chem.*, 2007, **50**, 2157.
14 W. Zhang, M.-P. Kung, S. Oya, C. Hou and H. F. Kung, *Nucl. Med. Biol.*, 2007, **34**, 89.

15 S. R. Choi, G. Golding, Z. Zhuang, W. Zhang, N. Lim, F. Hefti, T. E. Benedum, M. R. Kilbourn, D. Skovronsky and H. F. Kung, *J. Nucl. Med.*, 2009, **50**, 1887.
16 L. Yang, D. Rieves and C. Ganley, *N. Engl. J. Med.*, 2012, **367**, 885.
17 C. M. Clark, M. J. Pontecorvo, T. G. Beach, B. J. Bedell, R. E. Coleman, P. M. Doraiswamy, A. S. Fleisher, E. M. Reiman, M. N. Sabbagh, C. H. Sadowsky, J. A. Schneider, A. Arora, A. P. Carpenter, M. L. Flitter, A. D. Joshi, M. J. Krautkramer, M. Lu, M. A. Mintun and D. M. Skovronsky, *Lancet Neurol.*, 2012, **11**, 669.
18 M. Ono and H. Saji, *Int. J. Mol. Imaging*, 2011, 543267.
19 Z. Li, M. Cui, J. Dai, X. Wang, P. Yu, Y. Yang, J. Jia, H. Fu, M. Ono, H. Jia, H. Saji and B. Liu, *J. Med. Chem.*, 2013, **56**, 471.
20 J. L. Hickey and P. S. Donnelly, *Coord. Chem. Rev.*, 2012, **256**, 2367.
21 D. J. Hayne, S. Lim and P. S. Donnelly, *Chem. Soc. Rev.*, 2014, 6701.
22 X. Chen, P. Yu, L. Zhang and B. Liu, *Bioorg. Med. Chem. Lett.*, 2008, **18**, 1442.
23 R. Alberto, R. Schibli, P. A. Schubiger, U. Abram and T. A. Kaden, *Polyhedron*, 1996, **15**, 1079.
24 R. Alberto, K. Ortner, N. Wheatley, R. Schibli and A. P. Schubiger, *J. Am. Chem. Soc.*, 2001, **123**, 3135.
25 R. Alberto, R. Schibli, R. Waibel, U. Abram and A. P. Schubiger, *Coord. Chem. Rev.*, 1999, **190–192**, 901.
26 Y. Mikata, K. Takahashi, Y. Noguchi, M. Naemura, A. Ugai, S. Itami, K. Yasuda, S. Tamotsu, T. Matsuo and T. Storr, *Eur. J. Inorg. Chem.*, 2012, **2012**, 217.
27 S. R. Banerjee, M. K. Levadala, N. Lazarova, L. Wei, J. F. Valliant, K. A. Stephenson, J. W. Babich, K. P. Maresca and J. Zubieta, *Inorg. Chem.*, 2002, **41**, 6417.
28 C. Dumas, J. Petrig, L. Frei, B. Spingler and R. Schibli, *Bioconjugate Chem.*, 2005, **16**, 421.
29 N. Marti, B. Spingler, F. Breher and R. Schibli, *Inorg. Chem.*, 2005, **44**, 6082.
30 J. Giglio, G. Patsis, I. Pirmettis, M. Papadopoulos, C. Raptopoulou, M. Pelecanou, E. Leon, M. Gonzalez, H. Cerecetto and A. Rey, *Eur. J. Med. Chem.*, 2008, **43**, 741.
31 A. Chiotellis, C. Tsoukalas, M. Pelecanou, C. Raptopoulou, A. Terzis, M. Papadopoulos, Z. Papadopoulou-Daifoti and I. Pirmettis, *Inorg. Chem.*, 2008, **47**, 2601.
32 M. Patra, G. Gasser, D. Bobukhov, K. Merz, A. V. Shtemenko and N. Metzler-Nolte, *Dalton Trans.*, 2010, **39**, 5617.
33 L. A. Mullice, R. H. Laye, L. P. Harding, N. J. Buurma and S. J. A. Pope, *New J. Chem.*, 2008, **32**, 2140.
34 P. W. Causey, T. R. Besanger, P. Schaffer and J. F. Valliant, *Inorg. Chem.*, 2008, **47**, 8213.
35 S. R. Banerjee, J. W. Babich and J. Zubieta, *Inorg. Chem. Commun.*, 2004, **7**, 481.
36 S. R. Banerjee and J. Zubieta, *Acta Crystallogr., Sect. C: Cryst. Struct. Commun.*, 2005, **61**, m275.
37 D. D. Dischino, M. J. Welch, M. R. Kilbourn and M. E. Raichle, *J. Nucl. Med.*, 1983, **24**, 1030.
38 J. Meller and W. Becker, *Eur. J. Nucl. Med. Mol. Imaging*, 2002, **29**(Suppl 2), 38.
39 G. Lee and R. Bendayan, *Pharm. Res.*, 2004, **21**, 1313.
40 S. A. Hitchcock, *J. Med. Chem.*, 2012, **55**, 4877.
41 P. Kannan, V. W. Pike, C. Halldin, O. Langer, M. M. Gottesman, R. B. Innis and M. D. Hall, *Mol. Pharmaceutics*, 2013, **10**, 2222.
42 CrysAlis CCD, O. D. L. Version 1.171.32.5 (release 08-05-2007 CrysAlis171. NET; compiled May 8 2007, 13 : 10 : 02).
43 G. M. Sheldrick, *Acta Crystallogr., Sect. A: Found. Crystallogr.*, 2008, **64**, 112.
44 L. J. Farrugia, *J. Appl. Crystallogr.*, 1999, **32**, 837.
45 P. van der Sluis and A. L. Spek, *Acta Crystallogr.. Sect. A: Fundam. Crystallogr.*, 1990, **46**, 194.
46 J. Sutharsan, M. Dakanali, C. C. Capule, M. A. Haidekker, J. Yang and E. A. Theodorakis, *ChemMedChem*, 2010, **5**, 56.

